R. & M. No. 3509

MINISTRY OF TECHNOLOGY

AERONAUTICAL RESEARCH COUNCIL
REPORTS AND MEMORANDA

A Digital Computer Program for the Through-flow Fluid Mechanics in an Arbitrary Turbomachine using a Matrix Method

By H. Marsh

LONDON: HER MAJESTY'S STATIONERY OFFICE
1968

PRICE 15*s.* 0*d.* NET

A Digital Computer Program for the Through-flow Fluid Mechanics in an Arbitrary Turbomachine using a Matrix Method

By H. Marsh

Reports and Memoranda No. 3509*
July, 1966

Summary.
A detailed description is given of the development of a computer program for analysing the flow through axial, radial and mixed-flow turbomachines. The theory is based on the through-flow analysis given by *Wu*[1,2] and the equation for the stream function is solved by a matrix method. The theoretical predictions are compared with experiments reported by Jeffs[3] for a low-speed axial-flow compressor and it is shown that the theory gives a good estimate for the axial velocity profile.

LIST OF CONTENTS

*Replaces N.G.T.E. Report No. R. 282 – A.R.C. 28 246.

LIST OF ILLUSTRATIONS

1. *Introduction.*

There are several methods for estimating the flow through a turbomachine and the through-flow analysis is an attempt to obtain information about the overall flow pattern without including the effects of viscosity or time-dependent flows. The theory is based on the earlier work of Wu[1,2] and the through-flow analysis can be regarded as a simplified form of the general theory for the flow through an arbitrary turbomachine.

In the general theory[2], the equations of fluid motion are satisfied on two intersecting families of stream surfaces, the complete solution for the three-dimensional flow field being obtained by an iterative process between the flows on the two sets of surfaces. In all of the analysis, it is assumed that the flow relative to each blade row is steady. However, the flow and gas state at exit from a blade row vary circumferentially and the following blade row is then subject to a time-dependent inlet flow. The general method of analysis is therefore only applicable to the flow through an isolated blade row, or impeller channel, and even for these simple examples, the flow within the blade passage can only be estimated after specifying either the flow direction far downstream, or details of the flow at the trailing edge of the blades. The theory is general in the mathematical sense that it is a general method for estimating a steady three-dimensional flow by calculating the flow on the two sets of stream surfaces. In order to apply the general theory to estimate the flow through a multi-stage turbomachine, it would be necessary to remove the time dependence by circumferentially averaging the flow and the gas state between each pair of blade rows.

The through-flow theory is similar to the general theory, but the equations of fluid motion are only solved for the steady inviscid flow on a mean stream surface, and the blade thickness is still taken account of in that it affects the 'thickness' of this surface. The flow and gas state on this surface may be regarded as average values for the flow within the blade passage, a reasonable approximation when there are many blades. For a multi-stage turbomachine, the time dependence of the flow is removed by treating the through-flow solution as an axially symmetric flow for the duct region between each pair of blade rows.

The through-flow analysis for an isolated blade row does not require an assumption of axial symmetry. However, if axial symmetry is assumed, then the predicted flow pattern is the same as that which is obtained from the through-flow analysis for the flow on the mean stream surface. This point is discussed in more detail in Section 2.2. The advantage in not assuming axial symmetry is that the through-flow analysis can then be seen to be the first stage in the general theory and for an isolated blade row, or impeller, it is possible to continue the calculation to obtain the full three-dimensional flow field predicted by the general theory.

A computer program has been written to calculate the through-flow solution for a turbomachine of arbitrary shape. The program is sufficiently general to allow the flow pattern to be estimated for axial, radial and mixed-flow turbomachines and to demonstrate the use of the program, an example is given where the predictions of the theory can be compared with experimental results reported by Jeffs[3]. The current program is restricted to subsonic relative flow within blade passages, though this does not represent a limitation in principle to the method.

2. *The Through-flow Analysis.*

When analysing the flow through a turbomachine, it is convenient to express the equations in terms of the following quantities,

I	relative stagnation enthalpy, $I = H - \omega r V_u$,
H	stagnation enthalpy per unit mass,
r, z, ϕ	radial, axial and circumferential co-ordinates,
s	entropy per unit mass,
T	static temperature,

V_r, V_z, V_u radial, axial and circumferential velocity components,

W_r, W_z, W_u velocity components relative to a blade, $W_r = V_r$, $W_z = V_z$ and $W_u = V_u - \omega r$,

ρ static density,

ω angular velocity of a blade row.

The stagnation enthalpy H is measured in the fixed co-ordinate system, neglecting the gravitational force field, whereas I is the stagnation enthalpy measured by an observer in a co-ordinate system rotating with the blade row. In the rotating co-ordinate system there is a force field due to the rotation and this must not be neglected. The quantity I is the enthalpy of the fluid when brought to rest on the axis of rotation by a reversible adiabatic process. For an adiabatic flow, I remains constant along the streamlines in the rotating co-ordinate system, so that for any blade row,

$$I_{\text{in}} = I_{\text{out}}$$

or

$$H_{\text{in}} - H_{\text{out}} = (\omega r V_u)_{\text{in}} - (\omega r V_u)_{\text{out}}$$

This definition of the relative stagnation enthalpy is thus seen to be consistent with the Euler turbine equation. However, if T_{OR} is defined as the temperature of a perfect gas when brought to rest relative to the rotating co-ordinate system without any change in radial position by a reversible adiabatic process, then

$$T_{OR} = \left(I + \frac{\omega^2 r^2}{2}\right)/c_p$$

where c_p is the specific heat of the gas at constant pressure. In the presence of a radial force field, the product $c_p T_{OR}$ is not the relative stagnation enthalpy.

2.1. *The Derivation of the Principal Equation.*

In a co-ordinate system rotating with the blade at an angular velocity ω, any steady reversible, inviscid flow is governed by the equation of motion[2]

$$2\overline{\omega} \times \overline{W} - \overline{W} \times (\nabla \times \overline{W}) = -\nabla I + T\nabla s \tag{1}$$

where $\overline{W}$ is the relative velocity vector. In the r, z, ϕ co-ordinate system, the equations of continuity, motion, energy and state are

(a) *Continuity*

$$\frac{1}{r}\frac{\partial}{\partial r}(\rho r W_r) + \frac{1}{r}\frac{\partial}{\partial \phi}(\rho W_u) + \frac{\partial}{\partial z}(\rho W_z) = 0. \tag{2}$$

(b) *Motion*

$$-\frac{W_u}{r}\left[\frac{\partial}{\partial r}(rV_u) - \frac{\partial W_r}{\partial \phi}\right] + W_z\left[\frac{\partial W_r}{\partial z} - \frac{\partial W_z}{\partial r}\right] = -\frac{\partial I}{\partial r} + T\frac{\partial s}{\partial r} \tag{3}$$

$$\frac{W_r}{r}\left[\frac{\partial}{\partial r}(rV_u) - \frac{\partial W_r}{\partial \phi}\right] - W_z\left[\frac{1}{r}\frac{\partial W_z}{\partial \phi} - \frac{\partial W_u}{\partial z}\right] = -\frac{1}{r}\frac{\partial I}{\partial \phi} + \frac{T}{r}\frac{\partial s}{\partial \phi} \tag{4}$$

$$-W_r\left[\frac{\partial W_r}{\partial z} - \frac{\partial W_z}{\partial r}\right] + W_u\left[\frac{1}{r}\frac{\partial W_z}{\partial \phi} - \frac{\partial W_u}{\partial z}\right] = -\frac{\partial I}{\partial z} + T\frac{\partial s}{\partial z}. \tag{5}$$

(c) *Energy*

$$W_r \frac{\partial I}{\partial r} + \frac{W_u}{r} \frac{\partial I}{\partial \phi} + W_z \frac{\partial I}{\partial z} = \frac{DI}{Dt} = Q \tag{6}$$

where Q is the rate of heat addition per unit mass,

(d) *State* (perfect gas)

$$\rho = f(h, s) = A\, h^{\frac{1}{\gamma - 1}}\, e^{\left(-\frac{s}{R}\right)} \tag{7}$$

where h is the static enthalpy per unit mass.

A further equation for the entropy change along the streamlines can be obtained from Equations (3) to (6),

$$T\left[W_r \frac{\partial s}{\partial r} + \frac{W_u}{r} \frac{\partial s}{\partial \phi} + W_z \frac{\partial s}{\partial z} \right] = T \frac{Ds}{Dt} = Q\,. \tag{8}$$

These Equations, together with their boundary conditions, define the steady flow through any blade row or duct.

In general, these Equations have no simple solution and in the through-flow analysis, they are only solved for the flow on the mean stream surface. If this surface is defined as

$$S(r, z, \phi) = 0 \tag{9}$$

and $\bar{n}$ is the unit vector normal to the surface, then

$$\frac{n_r}{\dfrac{\partial S}{\partial r}} = \frac{n_u}{\dfrac{1}{r}\dfrac{\partial S}{\partial \phi}} = \frac{n_z}{\dfrac{\partial S}{\partial z}}. \tag{10}$$

For simplicity, it is assumed that the surface is single valued in ϕ,

$$\phi = \phi(r, z) \tag{11}$$

so that the two co-ordinates r and z are sufficient to define any point on the surface, the co-ordinate ϕ being obtained from Equation (11).

If $\overline{\dfrac{\partial q}{\partial r}}$ and $\overline{\dfrac{\partial q}{\partial z}}$ are partial derivatives taken along the stream surface, then

$$\left.\begin{aligned} \overline{\frac{\partial q}{\partial r}} &= \frac{\partial q}{\partial r} - \frac{n_r}{r n_u} \frac{\partial q}{\partial \phi} \\ \text{and} \quad \overline{\frac{\partial q}{\partial z}} &= \frac{\partial q}{\partial z} - \frac{n_z}{r n_u} \frac{\partial q}{\partial \phi} \end{aligned}\right\}. \tag{12}$$

These special derivatives are taken on the stream surface and must be distinguished from the ordinary partial derivatives. The special derivative $\frac{\overline{\partial q}}{\partial r}$ is the rate of change of q with r on the stream surface at a given value of z, whereas $\frac{\partial q}{\partial r}$ is the rate of change of q with r at given values of z and ϕ. It is only for an axially symmetric flow that the special derivatives become ordinary partial derivatives.

The equations governing the flow may now be expressed in terms of the special derivatives for the flow on the stream surface,

(a) *Continuity*

$$\frac{1}{r}\frac{\bar{\partial}}{\partial r}(\rho r W_r)+\frac{\bar{\partial}}{\partial z}(\rho W_z) = -\frac{\rho}{r n_u}\left[n_r\frac{\partial W_r}{\partial \phi}+n_u\frac{\partial W_u}{\partial \phi}+n_z\frac{\partial W_z}{\partial \phi}\right]$$

$$= \rho\, C(r,z)\,. \tag{13}$$

(b) *Motion*

$$-\frac{W_u}{r}\frac{\bar{\partial}}{\partial r}(rV_u)+W_z\left[\frac{\overline{\partial W_r}}{\partial z}-\frac{\overline{\partial W_z}}{\partial r}\right] = -\frac{\overline{\partial I}}{\partial r}+T\frac{\overline{\partial s}}{\partial r}+F_r \tag{14}$$

$$\frac{W_r}{r}\frac{\bar{\partial}}{\partial r}(rV_u)+\frac{W_z}{r}\frac{\bar{\partial}}{\partial z}(rV_u) = F_u \tag{15}$$

$$-W_r\left[\frac{\overline{\partial W_r}}{\partial z}-\frac{\overline{\partial W_z}}{\partial r}\right]-\frac{W_u}{r}\frac{\bar{\partial}}{\partial z}(rV_u) = -\frac{\overline{\partial I}}{\partial z}+T\frac{\overline{\partial s}}{\partial z}+F_z \tag{16}$$

where

$$\bar{F} = -\frac{1}{r\rho n_u}\frac{\partial p}{\partial \phi}.\bar{n}\,.$$

(c) *Energy*

For an adiabatic flow Equations (6) and (8) become

$$W_r\frac{\overline{\partial I}}{\partial r}+W_z\frac{\overline{\partial I}}{\partial z} = 0 \tag{17}$$

and

$$T\left[W_r\frac{\overline{\partial s}}{\partial r}+W_z\frac{\overline{\partial s}}{\partial z}\right] = 0\,. \tag{18}$$

In an inviscid flow, the force vector $\bar{F}$ is normal to the mean stream surface S and is therefore normal to the relative velocity vector,

$$W_r F_r+W_u F_u+W_z F_z = 0\,. \tag{19}$$

It is then convenient to introduce two angles λ' and μ' which define the local form of the stream surface,

$$\left.\begin{aligned} \operatorname{Tan}\lambda' &= \frac{n_r}{n_u} = \frac{F_r}{F_u} \\ \text{and}\qquad \operatorname{Tan}\mu' &= \frac{n_z}{n_u} = \frac{F_z}{F_u}. \end{aligned}\right\} \tag{20}$$

The three velocity components are then related by the Equation,

$$W_u = -W_r \operatorname{Tan}\lambda' - W_z \operatorname{Tan}\mu' \tag{21}$$

which is the geometrical condition that the flow follows the mean stream surface.

In order to obtain an equation for a stream function, Wu^2 introduces an integrating factor B, such that the equation of continuity becomes

$$\frac{\overline{\partial}}{\partial r}(rB\rho W_r)+\frac{\overline{\partial}}{\partial z}(rB\rho W_z) = 0. \tag{22}$$

The factor B is then related to $C(r, z)$ by

$$\frac{W_r}{B}\frac{\overline{\partial B}}{\partial r}+\frac{W_z}{B}\frac{\overline{\partial B}}{\partial z} = -C(r, z).$$

A stream function ψ may now be defined where

$$\left.\begin{aligned} \frac{\overline{\partial\psi}}{\partial r} &= rB\rho W_z \\ \text{and}\qquad \frac{\overline{\partial\psi}}{\partial z} &= -rB\rho W_r. \end{aligned}\right\} \tag{23}$$

The equations indicate that B is proportional to the local angular thickness of the stream surface and in the through-flow analysis, the thickness of the stream surface is assumed to be proportional to the width of the blade passage,

$$B = \frac{\text{circumferential width of the blade passage}}{\text{blade pitch}}$$

For flow in a duct region, where there are no blades, the parameter B is taken as unity.

If Equations (23) are substituted into the radial Equation of motion (14) then an equation for the stream function ψ is obtained,

$$\frac{\overline{\partial^2\psi}}{\partial r^2}+\frac{\overline{\partial^2\psi}}{\partial z^2} = \frac{\overline{\partial\psi}}{\partial r}\cdot\frac{\overline{\partial}}{\partial r}\left[\ln(r\rho B)\right]+\frac{\overline{\partial\psi}}{\partial z}\cdot\frac{\overline{\partial}}{\partial z}\left[\ln(r\rho B)\right]+$$

$$+\frac{r\rho B}{W_z}\left[\frac{\overline{\partial I}}{\partial r}-T\frac{\overline{\partial s}}{\partial r}-\frac{W_u}{r}\frac{\overline{\partial}}{\partial r}(rV_u)-F_r\right] \tag{24}$$

A similar equation can be obtained by substituting into the axial equation of motion,

$$\overline{\frac{\partial^2\psi}{\partial r^2}}+\overline{\frac{\partial^2\psi}{\partial z^2}}=\overline{\frac{\partial\psi}{\partial r}}\cdot\frac{\bar{\partial}}{\partial r}\left[\,ln(r\rho B)\,\right]+\overline{\frac{\partial\psi}{\partial z}}\cdot\frac{\bar{\partial}}{\partial z}\left[\,ln(r\rho B)\,\right]-$$

$$-\frac{r\rho B}{W_r}\left[\overline{\frac{\partial I}{\partial z}}-T\overline{\frac{\partial s}{\partial z}}-\frac{W_u}{r}\frac{\bar{\partial}}{\partial z}(rV_u)-F_z\right]. \tag{25}$$

The blade force components F_r and F_z are zero for a duct region, and within a blade row, they can be expressed as

$$F_r = F_u \operatorname{Tan}\lambda'$$

and

$$F_z = F_u \operatorname{Tan}\mu'$$

where F_u is given by Equation (15).

The two forms of *Wu*'s principal Equation, (24) and (25), have solutions which satisfy the equation of continuity, two of the three equations of motion and the energy Equation (17). If in addition, the entropy change is given by Equation (18), then this implies that the solution for the stream function satisfies all three equations of motion. It is therefore possible to use either form of the principal equation to obtain a solution for the stream function which satisfies the full set of equations governing the reversible flow on the mean stream surface.

The analysis has so far been confined to a system of axial and radial co-ordinates, but for some problems, it is convenient to rotate the axes through an angle θ, as shown in Figure 1. The two forms of the principal equation are then

$$\overline{\frac{\partial^2\psi}{\partial x^2}}+\overline{\frac{\partial^2\psi}{\partial y^2}}=\overline{\frac{\partial\psi}{\partial x}}\cdot\frac{\bar{\partial}}{\partial x}\left[\,ln(r\rho B)\,\right]+\overline{\frac{\partial\psi}{\partial y}}\cdot\frac{\bar{\partial}}{\partial y}\left[\,ln(r\rho B)\,\right]+$$

$$+\frac{r\rho B}{W_x}\left[\overline{\frac{\partial I}{\partial y}}-T\overline{\frac{\partial s}{\partial y}}-\frac{W_u}{r}\frac{\bar{\partial}}{\partial y}(rV_u)-F_y\right] \tag{26}$$

and

$$\overline{\frac{\partial^2\psi}{\partial x^2}}+\overline{\frac{\partial^2\psi}{\partial y^2}}=\overline{\frac{\partial\psi}{\partial x}}\cdot\frac{\bar{\partial}}{\partial x}\left[\,ln(r\rho B)\,\right]+\overline{\frac{\partial\psi}{\partial y}}\cdot\frac{\bar{\partial}}{\partial y}\left[\,ln(r\rho B)\,\right]-$$

$$-\frac{r\rho B}{W_y}\left[\overline{\frac{\partial I}{\partial x}}-T\overline{\frac{\partial s}{\partial x}}-\frac{W_u}{r}\frac{\bar{\partial}}{\partial x}(rV_u)-F_x\right]. \tag{27}$$

This rotation of the axes allows the through-flow analysis to be extended to a wide range of turbomachines.

Within a blade row, the geometry of the mean stream surface is defined in the xy co-ordinate system by the two angles λ and μ, where

$$\left.\begin{aligned}\operatorname{Tan}\lambda &= \frac{F_y}{F_u}\\ \text{and}\qquad \operatorname{Tan}\mu &= \frac{F_x}{F_u}.\end{aligned}\right\} \tag{28}$$

The three components of the relative velocity are related by

$$W_u = -W_y \operatorname{Tan} \lambda - W_x \operatorname{Tan} \mu \tag{29}$$

which corresponds to Equation (21).

The angle θ through which the axes are rotated is chosen to ensure that $W_x > 0$ throughout the region of flow and Equation (26) is expressed as

$$\overline{\frac{\partial^2 \psi}{\partial x^2}} + \overline{\frac{\partial^2 \psi}{\partial y^2}} = q(x, y) \tag{30}$$

where

$$q(x, y) = \overline{\frac{\partial \psi}{\partial x}} \cdot \frac{\bar{\partial}}{\partial x}\left[ln(r\rho\beta)\right] + \overline{\frac{\partial \psi}{\partial y}} \cdot \frac{\bar{\partial}}{\partial y}\left[ln(r\rho\beta)\right] +$$

$$+ \frac{r\rho\beta}{W_x}\left[\overline{\frac{\partial \alpha}{\partial y}} - T\overline{\frac{\partial s}{\partial y}} - \frac{W_u}{r}\frac{\bar{\partial}}{\partial y}(rV_u) - \gamma\right]$$

and α, β and γ have the following meanings,

(a) *Duct flow*

$$\alpha = H$$

$$\beta = 1$$

$$\gamma = 0 \text{ (no blades).}$$

(b) *Flow through a stator row*

$$\alpha = H$$

$$\beta = B$$

$$\gamma = F_y = F_u \operatorname{Tan} \lambda .$$

(c) *Flow through a rotor row*

$$\alpha = I = H - \omega r V_u$$

$$\beta = B$$

$$\gamma = F_y = F_u \operatorname{Tan} \lambda .$$

The principal Equation (26) is non-linear, but it can be solved by the repeated solution and correction of the quasi-linear Equation (30). A solution for ψ is obtained from Equation (30) for a given distribution $q(x, y)$, the function $q(x, y)$ is then corrected using the improved solution for ψ and the process is repeated until a convergence criterion is satisfied.

2.2. *The Assumption of Axial Symmetry.*

The through-flow analysis has been presented for the flow on the mean stream surface without assuming axial symmetry, so that this can be seen to be the first stage in applying the general theory[2]. However, if axial symmetry were assumed and a distributed body force introduced to represent the blade force, then the resulting principal equation for the stream function is of the same form as Equation (24), but with the special derivatives replaced by ordinary partial derivatives. It follows that the same flow pattern is obtained by assuming axial symmetry, or by solving for the flow on the mean stream surface and then treating this as an axially symmetric solution. The same solution is obtained irrespective of whether the assumption of axial symmetry is made before or after the equations are solved.

There is, however, an important difference between the through-flow and axially symmetric solutions. *Wu*[1] has pointed out that if axial symmetry is assumed and a body force introduced, then differentiating and combining the velocity components does not give the true vorticity. A close examination of the assumption of axial symmetry shows that this is equivalent to replacing the blade row by an 'actuator duct' where there are no blades, but the fluid is made to follow a certain surface by the application of a distributed body force. For a conducting fluid, this body force could be obtained by a magnetic field acting on a current flowing in the fluid. The assumption of axial symmetry is equivalent to forming an actuator duct model for the blade row and the inconsistency in calculating the vorticity arises from the use of the actuator duct model to represent the flow within the blade row. The through-flow analysis avoids this inconsistency by solving for the flow on the mean stream surface and by not assuming axial symmetry. The through-flow analysis only estimates the flow on the mean stream surface and the inconsistency in the calculation of vorticity is introduced by interpreting the solution as if it were axially symmetric.

2.3. *The Finite Difference Approximation.*

Many finite difference approximations use a rectangular grid of points, since this leads to simple expressions for the inter-dependence of the function values at neighbouring grid points. However, for calculating the flow through a turbomachine of arbitrary shape, a more suitable form of grid is a distorted, or non-rectangular mesh which is straight in only one direction. Figure 2 shows two types of distorted grid. In the quasiorthogonal grid the straight lines are chosen to lie approximately normal to the local direction of flow, while in the parallel grid, the straight lines are all parallel to the y axis. The quasi-orthogonal grid is well suited for calculating the flow through a turbomachine, but the parallel grid is adequate for many problems and requires less computer storage. The parallel grid was therefore chosen for the computer program to calculate the through-flow solution.

The distorted grid consists of m lines parallel to the y axis, each line having n equally spaced grid points between the inner and outer casings. By definition, the machine casings form curved grid lines so that there are no additional difficulties for grid points which lie close to the boundaries. The spacing of the parallel lines need not be uniform and where necessary, it can be varied locally. In the y direction, there is an automatic refining of the grid when the channel width is reduced.

The analysis has been presented in terms of *Wu*'s special derivatives for the flow on the mean stream surface. The distorted grid also lies on this surface, but in solving the principal Equation (30), the special derivatives do not introduce any additional complication and may be treated as normal partial derivatives.

The derivatives with respect to x and y at the mesh point (i,j) of Figure 3 can be expressed in terms of the function values at the neighbouring grid points, together with a truncation, or error, term which must be small. There is clearly no difficulty in forming the finite difference approximation for $\overline{\frac{\partial f}{\partial y}}$,

$$\left(\overline{\frac{\partial f}{\partial y}}\right)_{i,j} = \frac{f(i,j+1)-f(i,j-1)}{2k_0}+0[k_0^2]\,. \tag{31}$$

There are no simple general expressions for the derivatives in the x direction, but these can be formed in the following manner. A function α can be defined as

$$\alpha = \sum_{p,q} a_{pq} f(p, q) \tag{32}$$

where $f(p, q)$ is the function value at the grid point (p, q) which lies close to (i, j) and the coefficients a_{pq} are chosen so that α approximates the required derivatives to a suitable order of accuracy.

The principal Equation (30) is

$$\overline{\frac{\partial^2\psi}{\partial x^2}} + \overline{\frac{\partial^2\psi}{\partial y^2}} = q(x, y)$$

and the finite difference approximation for the Laplacian operator is obtained by choosing the coefficients a_{pq} such that

$$\alpha = \overline{\frac{\partial^2\psi}{\partial x^2}} + \overline{\frac{\partial^2\psi}{\partial y^2}} + 0\,[k_0^2]$$

where k_0 is the local spacing of the grid points in the y direction. When the Taylor series are substituted into Equation (32), there are ten conditions to be satisfied; the coefficients of ψ, $\overline{\frac{\partial\psi}{\partial x}}$, $\overline{\frac{\partial\psi}{\partial y}}$, $\overline{\frac{\partial^2\psi}{\partial x\partial y}}$, $\overline{\frac{\partial^3\psi}{\partial x^3}}$, $\overline{\frac{\partial^3\psi}{\partial x^2\partial y}}$, $\overline{\frac{\partial^3\psi}{\partial x\partial y^2}}$ and $\overline{\frac{\partial^3\psi}{\partial y^3}}$ must all be zero and the coefficients of $\overline{\frac{\partial^2\psi}{\partial x^2}}$ and $\overline{\frac{\partial^2\psi}{\partial y^2}}$ must be unity. In general, the Laplacian operator can be approximated by the function values at the ten points shown in Figures 3a and 3b. However, for certain conditions, there is more than one solution for a_{pq} and the method of solving for a_{pq} becomes ill-conditioned with singular matrices. This difficulty can be overcome by taking a different set of grid points on four grid lines, but this would increase the amount of computer storage required for the problem. An alternative solution is to relax the condition that the coefficient of $\overline{\frac{\partial\psi}{\partial x}}$ must be zero and to replace this by setting the coefficient of $\frac{\partial^4\psi}{\partial x^2\partial y^2}$ to zero. This is equivalent to expressing the principal equation in the form,

$$\begin{aligned}\overline{\frac{\partial^2\psi}{\partial x^2}} + \overline{\frac{\partial^2\psi}{\partial y^2}} + E\overline{\frac{\partial\psi}{\partial x}} &= q(x, y) + E\overline{\frac{\partial\psi}{\partial x}} \\ &= Q(x, y)\end{aligned} \tag{33}$$

where

$$E = 2\left[\frac{1}{(x_{i+1} - x_i)} - \frac{1}{(x_i - x_{i-1})}\right]$$

By using this form of the principal equation, there can never be any difficulty in evaluating the coefficients a_{pq} and the width of the resulting band matrix is minimised.

For most grid points, the function E is small, but it can be of the order $1/l$. In order to maintain an overall accuracy of the order, k_0^2, or l_1^2, or higher, it is necessary to develop a finite-difference approximation for $\overline{\frac{\partial \psi}{\partial x}}$ such that $E\overline{\frac{\partial \psi}{\partial x}}$ is calculated with sufficient accuracy. This approximation can be obtained by using the function values at the ten points shown in Figure 4 and choosing the coefficients a_{pq} so that

$$\alpha = \overline{\frac{\partial f}{\partial x}} + 0\left[l_1^3 \overline{\frac{\partial^4 f}{\partial x^4}}\right]$$

The finite-difference approximation for $E\overline{\frac{\partial \psi}{\partial x}}$ is then obtained to an accuracy $0[l_1^2]$, or higher. The first derivative with respect to x is required many times in the calculation and the coefficients a_{pq} are therefore stored for use with an Algol procedure which calculates $\overline{\frac{\partial f}{\partial x}}$ for any function f which is defined at the grid points. This procedure is used later in the program for calculating the function $Q(x, y)$.

2.4. *The Boundary Conditions.*

At inlet to the turbomachine, the three velocity components are given along with the stagnation enthalpy and density. The stream function is therefore defined for the first straight line of the grid, the upstream boundary. Since the inner and outer casings of the machine are also the limiting streamlines,

$$\psi(i, 1) = \psi(1, 1)$$

and

$$\psi(i, n) = \psi(1, n).$$

there being n grid points on each line. The downstream boundary condition is not easily defined when the flow is neither axial nor radial and for simplicity, it is assumed that the shape of the exit duct is such that the stream-function distribution is the same on the last two lines of the grid

$$\psi(m, j) = \psi(m-1, j)$$

there being m lines in the grid. For an axial flow machine, the exit duct should therefore have a constant hub to tip ratio and the grid should extend sufficiently far downstream for the flow to be almost axial.

2.5. *The Band Matrix Equation.*

The finite difference approximation for the principal Equation (33) and its boundary conditions can be written in the matrix form

$$[M].[\psi] = [Q] \tag{34}$$

where $[\psi]$ and $[Q]$ are the column vectors formed by $\psi(i, j)$ and $Q(i, j)$ and M is a band matrix. If the grid consists of m straight lines and n points per line, then the matrix $[M]$ has $(m-2)(n-2)$ rows and columns and the width of the band is $(2n-1)$. Only the band of non-zero elements is formed and stored in the computer. Equation (34) is solved by calculating the band triangular factors $[L]$ and $[U]$ where

$$[L].[M] = [U]$$

and then solving the Equation

$$[U]\ [\psi] = [L] \cdot [Q] \tag{35}$$

The matrices $[U]$ and $[L]$ are an upper band matrix and a lower triangular matrix respectively, but the information contained in $[L]$ is stored in the computer as a lower band matrix. The matrices $[U]$ and $[L]$ remain unchanged throughout the calculation. The subroutines for solving the band matrix equation were available as user-code subroutines for the KDF9 computer at the National Physical Laboratory.

2.6. *Limitations on the Grid Shape.*

It is difficult to give a general formula for the dependence of the truncation error on the local shape of the grid. However, it is clear that this error will increase as the grid is distorted from a square shape. The form of the grid suggests that the following limitations should be specified,

$$y(i-1,j+1) > y(i,j) > y(i-1,j-1)$$

and

$$y(i+1,j+1) > y(i,j) > y(i+1,j-1).$$

In practice, these conditions can always be satisfied by reducing the local spacing of the grid lines.

2.7. *Irreversible Flow.*

There are several methods for introducing the effects of irreversibility into the flow calculation. One simple method is to define two local polytropic efficiencies,

$$\eta_C = \frac{\Delta h_{is}}{\Delta h} \text{ for compression}$$

and

$$\eta_T = \frac{\Delta h}{\Delta h_{is}} \text{ for expansion}$$

where Δh_{is} is the change in enthalpy for an isentropic process having the same initial state as the actual process. The changes of entropy and enthalpy are then related by

$$\left.\begin{aligned} \frac{\Delta s}{R} &= \frac{\gamma}{\gamma-1}(1-\eta_C)\, ln\left(\frac{h+\Delta h}{h}\right) \\ \text{and} \quad \frac{\Delta s}{R} &= \frac{\gamma}{\gamma-1}\left(1-\frac{1}{\eta_T}\right) ln\left(\frac{h+\Delta h}{h}\right) \end{aligned}\right\} \tag{36}$$

For $\eta_C \leqslant 1$ and $\eta_T \leqslant 1$, one of these entropy changes is positive and the other is negative. But in an adiabatic flow, the entropy can only increase or remain constant in the direction of flow. The computer program is therefore made to examine the local change of enthalpy along the streamline and to take the appropriate positive increase in entropy.

The local polytropic efficiencies are used as a simple method for relating the local changes of enthalpy and entropy and they are not used elsewhere in the calculation. The procedure for calculating the entropy is a self-contined section of the program and it can easily be replaced by an alternative method for estimating the entropy change.

This method of introducing the effect of irreversibility is basically inconsistent in that the equations of motion remain those for a reversible flow. It is possible to avoid this inconsistency by including small frictional forces in the equations of motion, but at present, there is no reliable method for estimating these forces.

3. *The Method of Solution.*

The method of solving the modified principal Equation (34) for the stream function ψ is to solve for a given vector $[Q]$, to correct $[Q]$ using the new flow pattern and then to repeat the cycle of calculation until a criterion of convergence is satisfied. Whilst this is an accurate description of the overall method of solution, there are several points of detail which require further explanation and these will now be considered.

3.1. *The Calculation of the Gas State.*

The variations of the velocity components and the gas state through the machine are obtained by tracing the local streamline pattern. The solution for the stream function ψ defines the streamline pattern and by differentiating ψ with respect to x and y, it is possible to calculate the products ρV_y and ρV_x at each grid point. The flow and the gas state are defined at the upstream boundary, the first line of the grid, and the solution for the gas state and flow may be extended line by line through the grid. The streamline passing through the grid point C on the grid line i of Figure 5a is traced back to the point A on the previous grid line, where the flow and the gas state are already known. The method for calculating the flow at C is dependent on the location of C and takes one of the following forms:

(a) *Duct flow*

If the point C lies in a duct region, then there is no change of stagnation enthalpy or angular momentum along the streamline AC,

$$H_C = H_A$$

and

$$(rV_u)_C = (rV_u)_A .$$

Equation (7) for the density can be expressed in the form

$$\frac{\rho}{\rho_0} = \left(\frac{h}{H_0}\right)^{\frac{1}{\gamma-1}} e^{\left(\frac{s_0-s}{R}\right)} \tag{37}$$

where the subscript 0 refers to the stagnation state far upstream of the machine. Equation (37) can be arranged as

$$\Sigma = \left(1-\frac{\Phi}{\Sigma^2}\right)^{\frac{1}{\gamma-1}} \tag{38}$$

where

$$\Sigma = \frac{\rho}{\rho_0}\left(\frac{H_0}{H-\frac{V_u^2}{2}}\right)^{\frac{1}{\gamma-1}} e^{\left(\frac{s-s_0}{R}\right)} \tag{39}$$

and

$$\Phi = \left[\frac{(\rho V_x)^2+(\rho V_y)^2}{2\rho_0^2 H_0}\right]\left(\frac{H_0}{H-\frac{V_u^2}{2}}\right)^{\frac{\gamma+1}{\gamma-1}} e^{2\left(\frac{s-s_0}{R}\right)} \tag{40}$$

For a given value of Φ, the solution of Equation (38) for Σ is obtained by referring to a table of corresponding values of Φ and Σ which is stored in the computer. This is far simpler and quicker than solving Equation (38) by a Newton-Raphson process and it avoids any difficulty with convergence. When Σ is known then the density can be calculated from Equation (39), it being assumed that the entropy is already known, or can be estimated.

It is possible that on an early iteration, $\Phi > \Phi_{max}$ at some point, which indicates that the solution for ψ has not yet converged. For this condition, there is no real value of Σ to satisfy Equation (38) and the computer program sets $\Phi = \Phi_{max}$, prints out a warning message and continues with the calculation.

(b) *Stator row*

If C lies within a stator row, then there is no change of stagnation enthalpy between the points A and C.

$$H_C = H_A$$

At C the flow must lie on the mean stream surface and the velocity component V_u is given by

$$V_u = -V_y \operatorname{Tan} \lambda - V_x \operatorname{Tan} \mu$$

or

$$(\rho V_u) = -(\rho V_y) \operatorname{Tan} \lambda - (\rho V_x) \operatorname{Tan} \mu . \tag{41}$$

The equation for the density can again be expressed in the form

$$\Sigma = r\left(1 - \frac{\Phi}{\Sigma^2}\right)^{\frac{1}{\gamma-1}}$$

but the definitions of Φ and Σ are now

$$\Sigma = \frac{\rho}{\rho_0}\left(\frac{H_0}{H}\right)^{\frac{1}{\gamma-1}} e^{\left(\frac{s-s_0}{R}\right)} \tag{42}$$

and

$$\Phi = \left[\frac{(\rho V_x)^2 + (\rho V_y)^2 + (\rho V_u)^2}{2\rho_0^2 H_0}\right]\left(\frac{H_0}{H}\right)^{\frac{\gamma+1}{\gamma-1}} e^{2\left(\frac{s-s_0}{R}\right)}. \tag{43}$$

For a given value of Φ, the corresponding value of Σ is obtained from the Φ, Σ table and the density may then be calculated from Equation (42). When the density is known, then it is possible to calculate the three velocity components at C. The method of calculation assumes that the entropy is already known and this will be discussed later in more detail.

(c) *Rotor row*

If C lies within a rotor row, then the relative stagnation enthalpy I remains constant along the streamline AC,

$$H_C = H_A + \omega_C \left[(rV_u)_C - (rV_u)_A\right]. \tag{44}$$

Since C lies within a blade row, the flow at C must lie on the mean stream surface and the product ρW_u is given by

$$\rho W_u = -(\rho V_y) \operatorname{Tan} \lambda - (\rho V_x) \operatorname{Tan} \mu . \tag{45}$$

As before the density Equation can be written in the form

$$\Sigma = \left(1 - \frac{\Phi}{\Sigma^2}\right)^{\frac{1}{\gamma-1}}$$

where Σ and Φ are now given by

$$\Sigma = \frac{\rho}{\rho_0}\left(\frac{H_0}{I + \frac{\omega^2 r^2}{2}}\right)^{\frac{1}{\gamma-1}} e^{\left(\frac{s-s_0}{R}\right)} \tag{46}$$

and

$$\Phi = \left[\frac{(\rho V_x)^2 + (\rho V_y)^2 + (\rho W_u)^2}{2\rho_0^2 H_0}\right]\left(\frac{H_0}{I + \frac{\omega^2 r^2}{2}}\right)^{\frac{\gamma+1}{\gamma-1}} e^{2\left(\frac{s-s_0}{R}\right)}. \tag{47}$$

It is thus seen that the Φ, Σ table can be used again to obtain the value of Σ and the density can then be calculated from Equation (46). When the density is known then the three velocity components and the stagnation enthalpy can be calculated at the point C.

The use of the Φ, Σ table for calculating the density was described by *Wu*[2] and it is an important feature of this computer program. The solution of the density equation is required several thousand times in a single problem and it is therefore important to have a method of solution which is fast and cannot diverge. The tabular method meets these requirements. The Φ, Σ table is formed by the program using the formula

$$\Phi = \Sigma^2 - \Sigma^{\gamma+1}$$

where γ is the ratio of the specific heats for the gas. If the fluid is incompressible, then the density is set to ρ_0 at all points in the grid.

When calculating the density at the point C, it is assumed that the entropy at C is known. It is possible to calculate the density and enthalpy for a given value of entropy and then to correct the entropy and to repeat the cycle of calculation until the process converges. In practice this is not necessary and the method for estimating the density can be based on the entropy field calculated on the previous iteration. When the flow and the gas state at C are known, then a value is calculated for the entropy at C and this is used on the next iteration. The calculation of the entropy therefore lags one iteration behind the main calculation, but as the solution for ψ converges the error due to this lag disappears.

3.2. *The Trailing Edge.*

In general, the trailing edge of a blade row does not coincide with a grid line and it is then difficult to estimate the flow downstream of the blade row. In Figure 5b the streamline passing through the grid point C is traced back to the point A on the previous grid line and B is the intersection of the streamline with the trailing edge. It is assumed that the gas state and the derivatives of the stream function are locally linear, so that

$$\rho_B = \frac{BC}{AC}\rho_A + \frac{AB}{AC}\rho_C. \tag{48}$$

Since it is necessary to specify the position of B before the streamline pattern is known, it is assumed that

$$\frac{AB}{AC} \simeq \frac{DE}{DC}$$

where DC is the curved grid line which intersets the trailing edge at E. This is a simple method for estimating the flow at the trailing edge, which need not be straight, and it allows the calculation of the gas state to pass from a blade row to a duct region.

When estimating the flow at the trailing edge, there is a further difficulty in that the gas state at C is not yet known for the current iteration. The program therefore uses the gas state at C from the previous iteration when calculating the flow at the trailing edge. The error due to this approximation is reduced as the solution for ψ converges.

3.3. *The Mach Number Limitations.*

Wu[2] has shown that the condition for the principal equation to remain elliptic is

(a) if the angular momentum is specified,

$$rV_u = G(x, y),$$

then

$$M_m < 1$$

where M_m is the meridional Mach number,

$$M_m = \frac{\sqrt{V_x^2 + V_y^2}}{c}$$

c being the local velocity of sound in the gas,

(b) if the velocity components are related by

$$W_u = -V_y \operatorname{Tan} \lambda - V_x \operatorname{Tan} \mu$$

$$= g(V_x, V_y)$$

then

$$M_{\text{rel}} < 1$$

where M_{rel} is the relative Mach number,

$$M_{\text{rel}} = \frac{\sqrt{V_x^2 + V_y^2 + W_u^2}}{c}.$$

It can also be shown that the equation used for calculating the density

$$\Sigma = \left(1 - \frac{\Phi}{\Sigma^2}\right)^{\frac{1}{\gamma - 1}}$$

has two solutions for Σ, one for $M_m < 1$, or $M_{\text{rel}} < 1$, and the other for $M_m > 1$, or $M_{\text{rel}} > 1$, To avoid ambiguity and to ensure that the principal equation remains elliptic, the computer program is restricted to flows where at each grid point

(a) if $G(x, y)$ is given, then $M_m < 1$

(b) if $g(V_x, V_y)$ is given, then $M_{\text{rel}} < 1$.

It should be noted that the Mach number limitation is determined by the method of calculating the circumferential velocity component rather than by the physical location of the grid point. If the grid point lies immediately downstream of the trailing edge and $g(V_x, V_y)$ is given as though the point lay at the trailing edge then M_{rel} must be less than unity, even though the grid point lies within a duct region.

3.4. *The Relaxation Factor and Convergence.*

When Equation (35) has been solved for ψ, the new stream function for the k^{th} iteration is defined by

$$\psi_k = \psi_{k-1} + \alpha(\psi - \psi_{k-1})$$

The parameter α is a relaxation factor which is chosen to improve the stability of the iterative process, or to improve the convergence. The stability can be further improved by limiting the maximum change in the local value of the stream function on successive iterations,

$$|\psi_k - \psi_{k-1}| < \beta|\psi_{k-1}|$$

and

$$|\psi_k - \psi_{k-1}| < \beta|\psi(1, n) - \psi_{k-1}|$$

$\psi(1, n)$ being a boundary condition. The through-flow analysis is based on the assumption that there are no regions of reverse flow and the two limitations on $|\psi_k - \psi_{k-1}|$ do not add any further restriction to the analysis. A typical value for β is 0·1 and α normally lies in the range 0·25 to 1·0. The local value of the effective relaxation factor is always less than, or equal to α, but it becomes equal to α as the solution for ψ converges. The criterion for convergence is that

$$\left| \frac{\psi - \psi_{k-1}}{\psi_{k-1}} \right| < \gamma$$

at all points in the grid, typical values for γ being 0·001 or 0·0001. This order of accuracy is normally obtained within 10 to 20 iterations.

4. *The Computer Program.*

The computer program is written in two parts with a private magnetic tape being used to transfer information to the second program. The first program forms the distorted grid, the finite difference approximations, the band matrix $[M]$ and the band triangular factors $[U]$ and $[L]$. The grid data, the band matrices $[U]$ and $[L]$ and the coefficients for calculating the first derivative with respect to x are then stored on the magnetic tape. The second program reads back this information from the magnetic tape and then calculates the flow through the turbomachine. The use of magnetic tape allows the second program to be used separately, the basic data for a given turbomachine remaining stored on the magnetic tape. The second program performs the remaining calculations for any given set of boundary conditions.

The programs are written in Algol for an English Electric KDF9 computer having a high speed store of 32K words. The programs each have a typical operating time of 3 to 7 minutes and the size of problem which can be analysed is limited to

$$mn(3n+21) < 21{,}000 \text{ approx.}$$

where the grid consists of m straight lines with n points per line. Recent developments in the use of magnetic tape storage when solving band matrix equations should allow the program to be extended to deal with larger problems.

In the following example $m = 38$ and $n = 7$ making $mn(3n+21) = 11{,}172$ which is about half the maximum value quoted for a 32K word store.

5. *A Comparison between Theroy and Experiment.*

A detailed description of the full range of problems which has been investigated using this program, is beyond the scope of this Report. Instead one example is given where there is sufficient experimental data to permit a detailed comparison with the theoretical predictions. The experiments, which have been reported by Jeffs[3], were performed on a low speed single stage axial flow compressor of constant hub to tip ratio. The overall layout of the compressor is shown in Figure 6, the axial velocity profile being measured at the planes *A*, *B*, *C* and *D*. Full details of the blading are given in Reference 3 and this is summarised in Table I. The hub radius of the machine was 5 in., the tip radius was 10 in. and the rotational speed was 1,375 rev/min. The comparison between theory and experiment is made for three mass flow rates corresponding to

$$\frac{\overline{V_a}}{U_m} = 0{\cdot}58 \text{ (surge point)}$$

$$\frac{\overline{V_a}}{U_m} = 0{\cdot}65 \text{ (design value is } 0{\cdot}62)$$

$$\frac{\overline{V_a}}{U_m} = 0{\cdot}75\,,$$

these being the values reported by Jeffs[3].

The theoretical predictions were made for a grid consisting of 38 radial straight lines with 7 equally spaced points on each line, there being 10 lines upstream of the inlet guide vanes, 3 lines within each blade row, 3 lines between each pair of blade rows and 13 lines in the downstream duct. The grid extended from 2·1 blade heights ahead of the inlet guide vanes, to 2·9 blade heights downstream of the stator row, as shown in Figure 6. The calculations were made for a compressible flow using the design air angles given by Jeffs. The flow pattern was estimated for a reversible flow, $\eta_C = \eta_T = 1$ at all points, and also for an irreversible flow, $\eta_C = \eta_T = 0{\cdot}9$ at all points, these being arbitrary values for the polytropic efficiencies which were chosen to show the overall effect of irreversibility. It is difficult to estimate the correct values for the local polytropic efficiencies, since the analysis requires information about the local changes in entropy within the blade row, whereas all the experimental data relate to the behaviour of complete blade rows.

The experimental and theoretical axial velocity profiles are compared in Figures 7 to 18 for the three mass flow rates. In all three examples, there is good agreement between the experimental results and the predictions for the reversible flow through the inlet guide vanes and the rotor row and the agreement is improved by introducing the effect of irreversibility. At exit from the stator and far downstream, good agreement between the reversible flow and the experiments is only obtained at the highest mass flow rate, $\frac{\overline{V_a}}{U_m} = 0{\cdot}75$. At the lowest mass flow rate, the agreement with the reversible flow calculation is only fair, but again the introduction of irreversibility is seen to improve the agreement. According to Jeffs[3], the lowest mass flow rate corresponds to the onset of surge and the stator blades are probably stalled at the tip section.

It is clear from the comparisons that the effect of irreversibility becomes more important as the flow passes through more blade rows; this is a cumulative effect. There is little difference between the reversible and irreversible flows through the inlet guide vanes, but on passing through the rotor and stator rows, the entropies at the hub and tip radii increase rapidly and there is a large difference in the velocity profiles at the downstream position.

The comparisons show that the through-flow analysis can give a good estimate for the flow in an axial-flow compressor. The agreement between the theoretical and experimental profiles is good, but it should not be difficult to improve on these results, particularly at the hub and tip sections, by allowing for the variation of loss and air exit angle with incidence and by including the effect of secondary flow. The comparisons have been made for a compressor which was designed for a radially constant axial velocity at $\frac{\overline{V_a}}{U_m} = 0{\cdot}62$. Since this condition was not obtained, the comparisons are therefore made for 'off-design' operation and better agreement would probably be obtained for a machine which was designed on the basis of the through-flow analysis.

6. *Conclusions.*

The matrix through-flow analysis has been known for many years, but the lack of suitable large computers has prevented the application of the theory. *Wu*[2] described the method for developing a computer program and in this Report a detailed description has been given of a program which can be used to analyse the flow through a wide range of turbomachines. The present work makes several contributions to the general problem of estimating the flow in a turbomachine. There are few restrictions on the shape of the inner and outer casings; the calculations are now extended to the flow within the blade rows and the effects of blade thickness and taper have both been included in the theory. No simplifying assumptions have been made about the magnitude of the radial blade force component and the program can be used to analyse machines with blades which are not radial.

The comparisons with the experimental results of Jeffs[3] show that the through-flow analysis can give a good estimate for the axial velocity profile in an axial flow compressor. The use of two polytropic efficiencies allows the overall effect of irreversibility to be demonstrated and it is hoped that further work may lead to better methods for introducing and distributing the losses which occur in turbomachines. Previous methods of analysis have been able to use experimental data on the behaviour of complete blade rows, but with the through-flow method detailed information is now required about the flow within the blade rows.

The through-flow program requires a computer with a large high speed store which may prevent a wider application of this method of analysis. It may be necessary to develop an alternative method for solving the through-flow equations which does not require such a large computer. However, the project has shown that this is a useful method of analysis, that the flow can be calculated within the blade rows and that a general program can be written to analyse the flow in axial, radial and mixed-flow turbomachines. It will be recalled that a Mach number limitation exists in the current program which is mentioned in Sections 1 and 3.3.

Acknowledgements.

The author would like to thank Mrs. G. Peters and Mrs. M. Price of the National Physical Laboratory for their advice and help in the development of this program.

LIST OF SYMBOLS

B	Integrating factor, or surface thickness parameter
c	Local velocity of sound
C	Function defined by Equation (13)
c_p	Specific heat by constant pressure
E	Function defined by Equation (33)
F	Force vector
g, G	Functions apparent from the text
h	Static enthalpy per unit mass
H	Stagnation enthalpy per unit mass
I	Relative stagnation enthalpy per unit mass $I = H - \omega r V_u$
k	Local spacing of the grid points in the y direction
l	Local spacing of the grid lines in the x direction
$[L]$	Lower band matrix
m	Number of straight lines in the grid
$[M]$	Band matrix
M_m	Meridional Mach number
M_{rel}	Relative Mach number
n	Number of points on each grid line
$\bar{n}$	Vector normal to the mean stream surface
q	Function defined by Equation (30)
Q	Function defined by Equation (33)
$[Q]$	Column vector formed by $Q(\bar{i},\bar{j})$
r	Radius
R	Gas constant
s	Entropy per unit mass
S	Mean stream surface, $S(r, z, \phi) = 0$
t	Time
T	Temperature
U_m	Blade speed at the mean radius
$[U]$	Upper band matrix
$\bar{V}$	Velocity vector
V_a	Axial velocity

$\overline{V}_a$	Mean axial velocity
$\overline{W}$	Relative velocity vector
x, y	co-ordinates with tilted axes
z	Axial distance
γ	Ratio of specific heats
η_C	Polytropic efficiency for compression
η_T	Polytropic efficiency for expansion
θ	Angle between the zr and xy co-ordinate systems
λ, μ	Angles which define the local shape of the mean stream surface
ρ	Density
Σ	Variable used in calculating the density
ϕ	Circumferential co-ordinate
Φ	Variable used in calculating the density
ψ	Stream function
$[\psi]$	Column vector formed by $\psi(i,j)$
ω	Angular velocity of the blade

Subscripts

0	Stagnation state far upstream
r	Radial
u	Circumferential
x	x component
y	y component
z	z component

Superscript

$\frac{\overline{\partial}}{\partial x}$ or $\frac{\overline{\partial}}{\partial y}$	derivatives taken along the mean stream surface

REFERENCES

No.	*Author(s)*	*Title, etc.*
1	C.–H. Wu	A general through-flow theory of fluid flow with subsonic or supersonic velocity in turbomachines of arbitrary hub and casing shapes. N.A.C.A. TN 2302, 1951.
2	C.–H. Wu	A general theory of three-dimensional flow in subsonic and supersonic turbomachines of axial, radial and mixed-flow types. N.A.C.A. TN 2604, 1952.
3	R. A. Jeffs	The low speed performance of a single stage of twisted constant section blades at a diameter ratio of 0·5. N.G.T.E. Memorandum No. M.206, A.R.C. 17 081, March 1954. *See* also *Incompressible Aerodynamics* (Edited by B. Thwaites) p. 494. Oxford University Press.

TABLE I

*C.*123 *compressor*

Relative-air Angles at Blade Exit (*degrees*)

Radius (in.)	5·0	5·8$\dot{3}$	6·6$\dot{6}$	7·5	8·3$\dot{3}$	9·1$\dot{6}$	10·0
I.G.V.	8·5	16·5	21·6	25·6	28·5	30·8	32·2
Rotor	−3·7	7·0	16·7	25·6	33·4	40·1	45·5
Stator	8·5	16·5	21·6	25·6	28·5	30·8	32·2

(all angles measured relative to the axial direction)

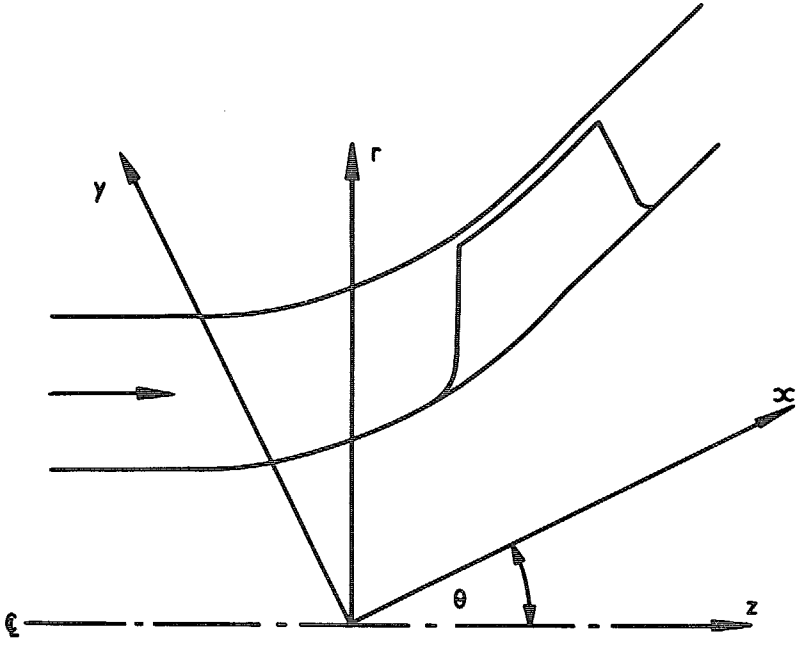

FIG. 1. The xy co-ordinate system.

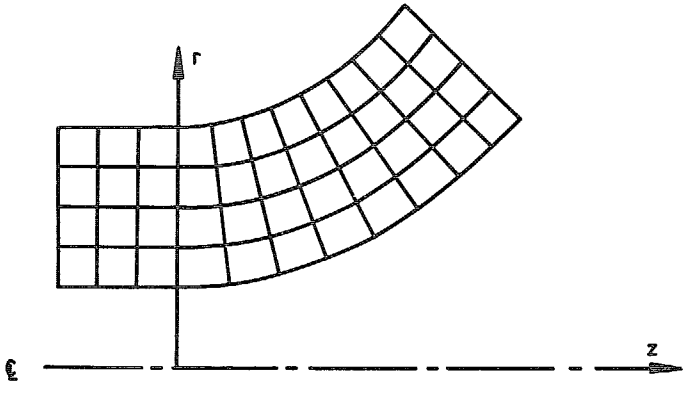

a) QUASI-ORTHOGONAL GRID

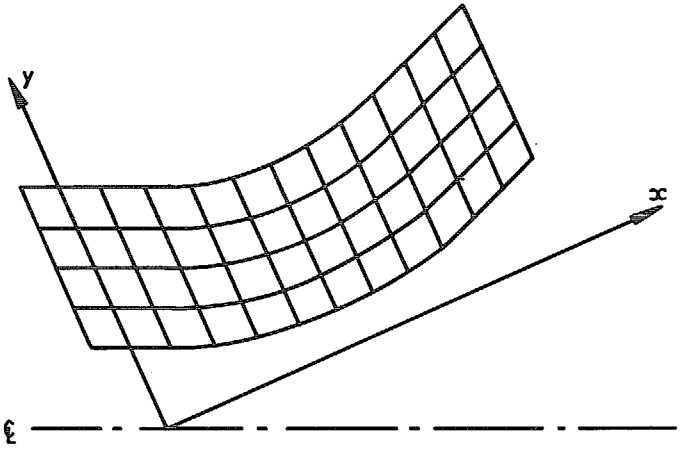

b) PARALLEL GRID

FIG. 2a and b. A choice of grids.

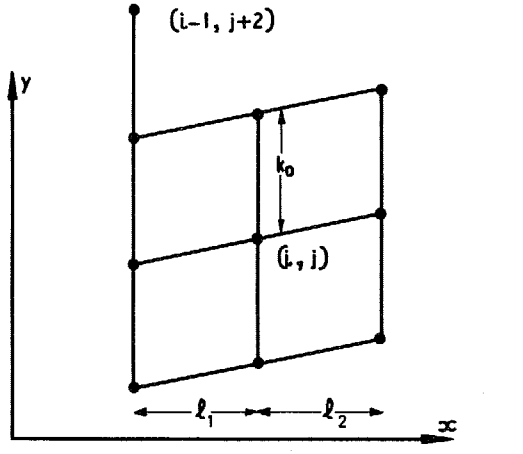

a) GRID FOR $1<j<n-1$

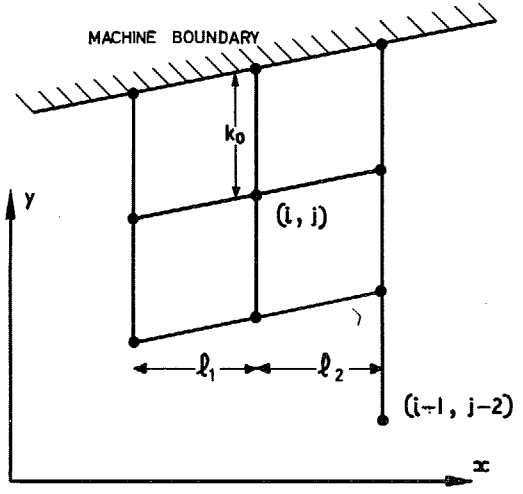

b) GRID FOR $j=n-1$

FIG. 3a and b. Finite-difference grids.

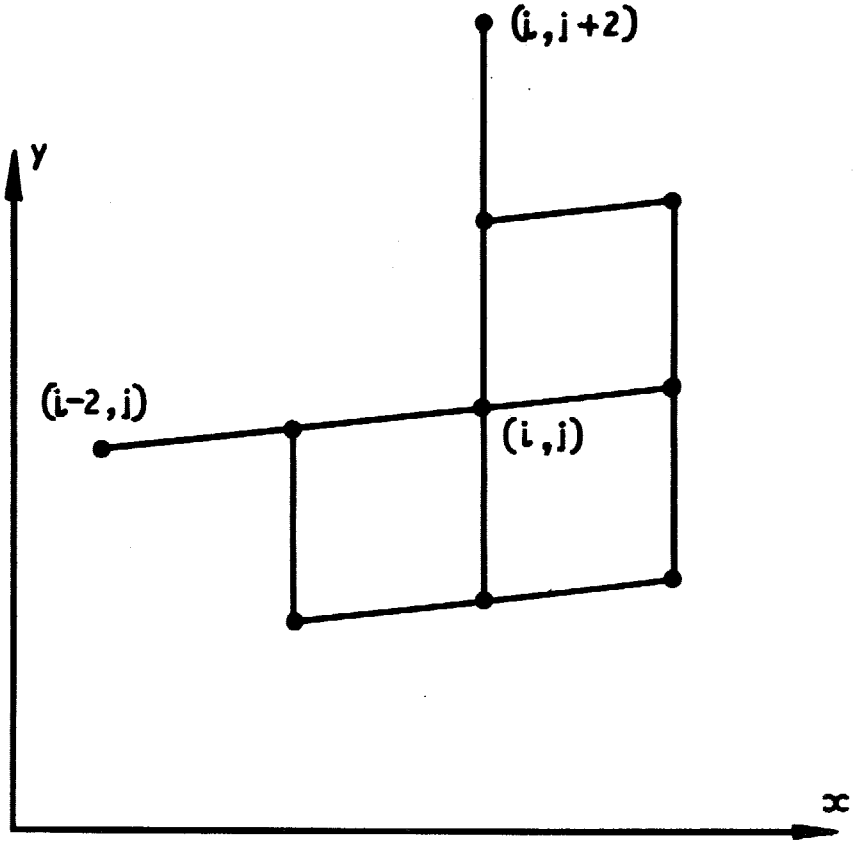

FIG. 4. The basic 10-point grid for $\overline{\frac{\partial f}{\partial x}}$.

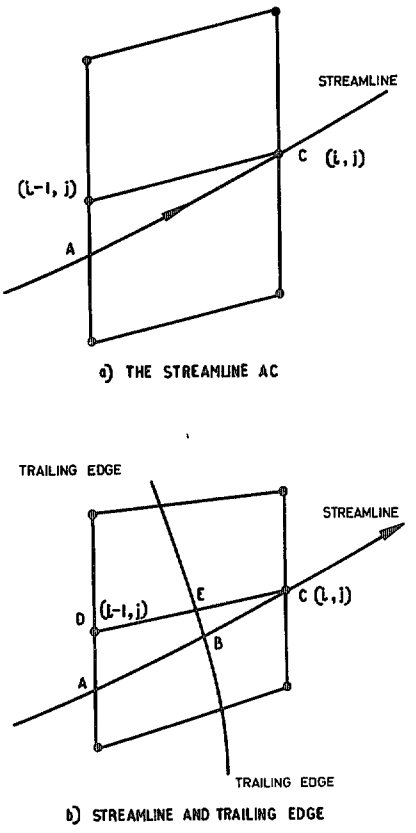

FIG. 5a and b. Streamline intercepts.

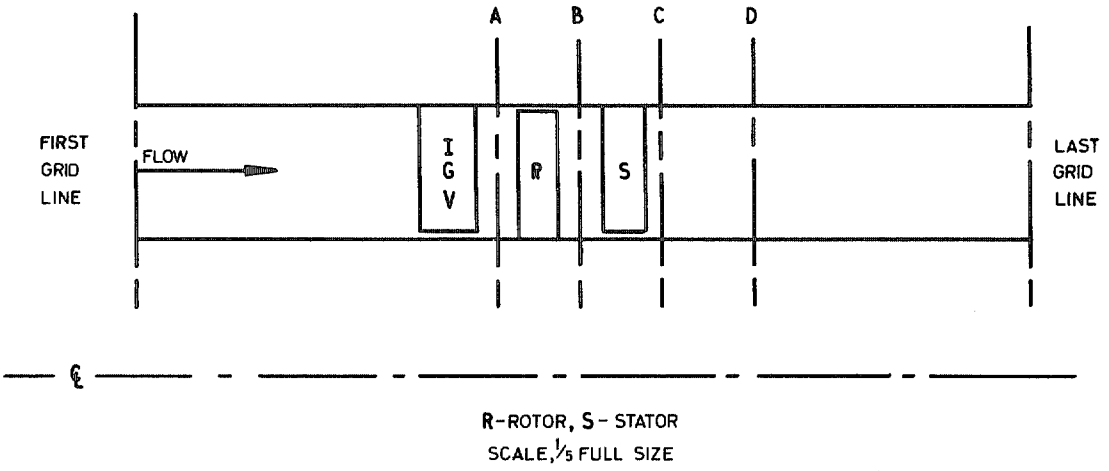

FIG. 6. C.123 Compressor.

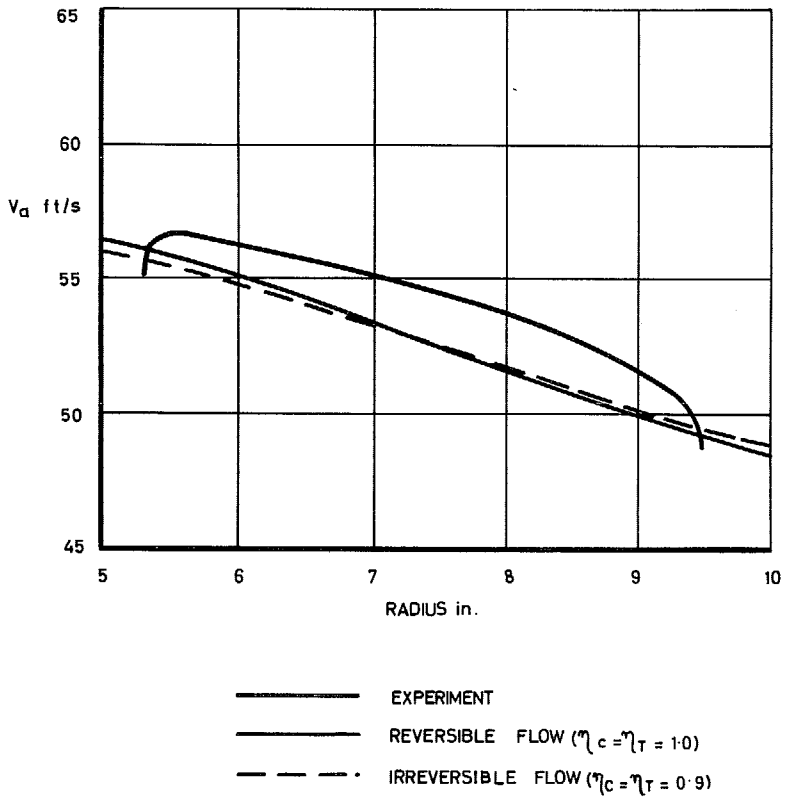

FIG. 7. Axial velocity profile after *IGV*, $\bar{V}_a/U_m = 0{\cdot}58$.

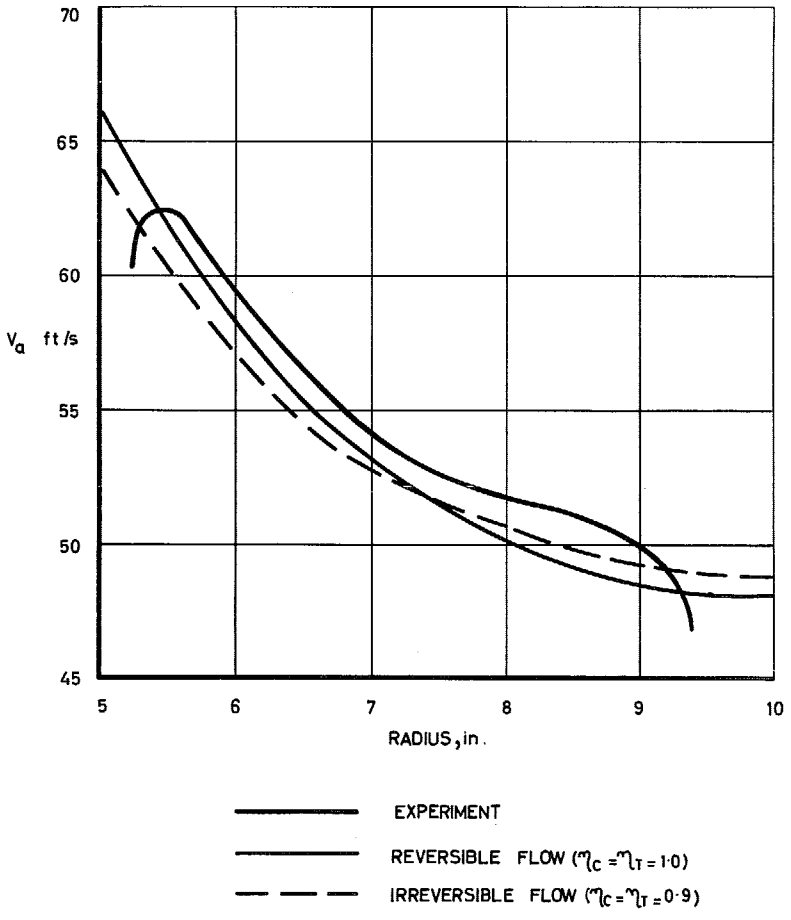

FIG. 8. Axial velocity profile after rotor, $\bar{V}_a/U_m = 0{\cdot}58$.

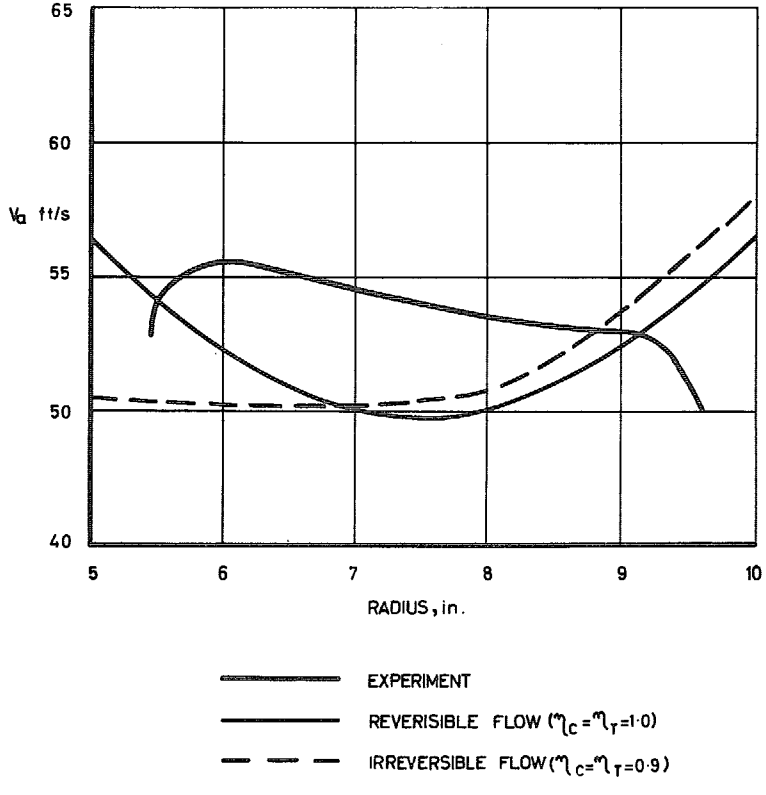

FIG. 9. Axial velocity profile after stator, $\overline{V}_a/U_m = 0{\cdot}58$.

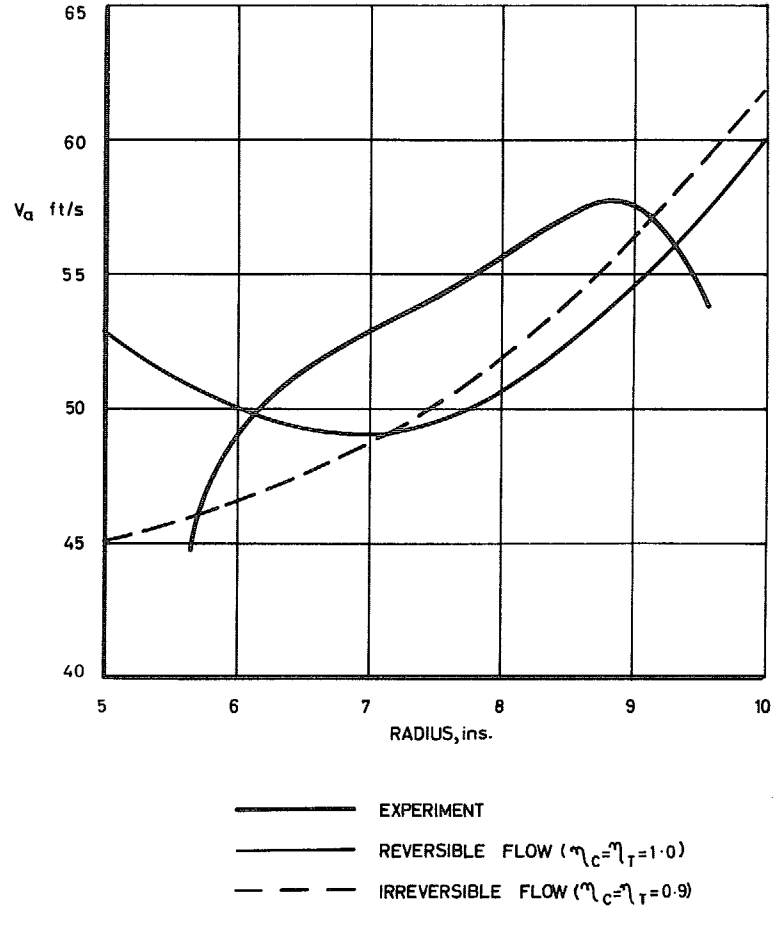

FIG. 10. Axial velocity profile far downstream $\overline{V}_a/U_m = 0{\cdot}58$.

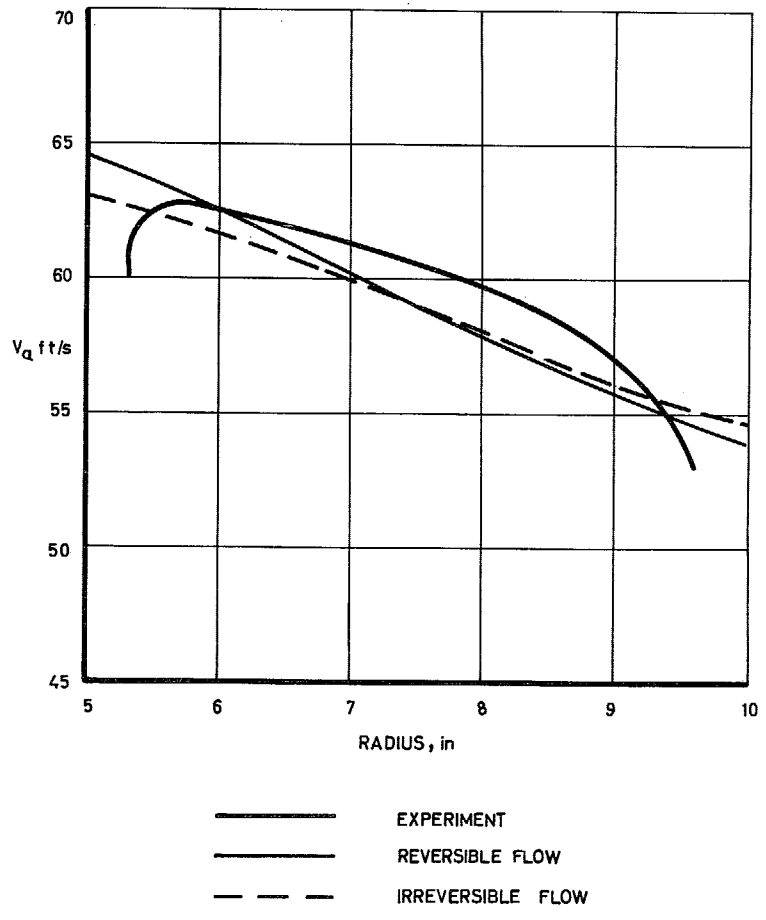

FIG. 11. Axial velocity profile after *IGV*, $\bar{V}_a/U_m = 0{\cdot}65$.

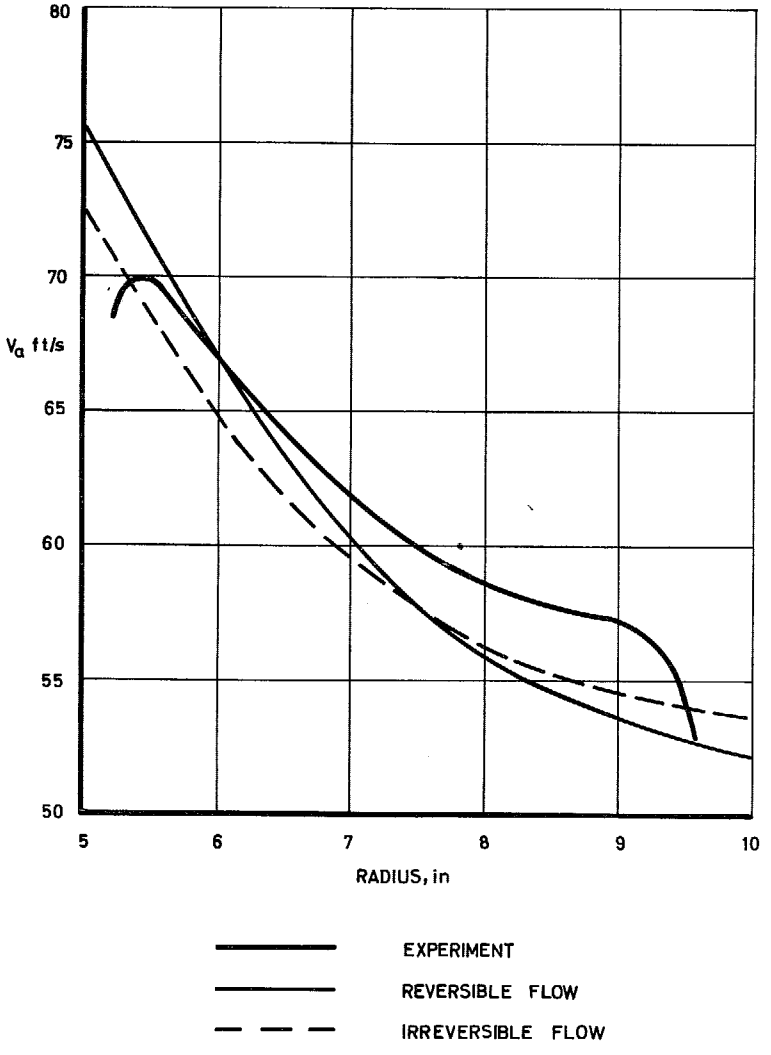

FIG. 12. Axial velocity profile after rotor, $\bar{V}_a/U_m = 0{\cdot}65$.

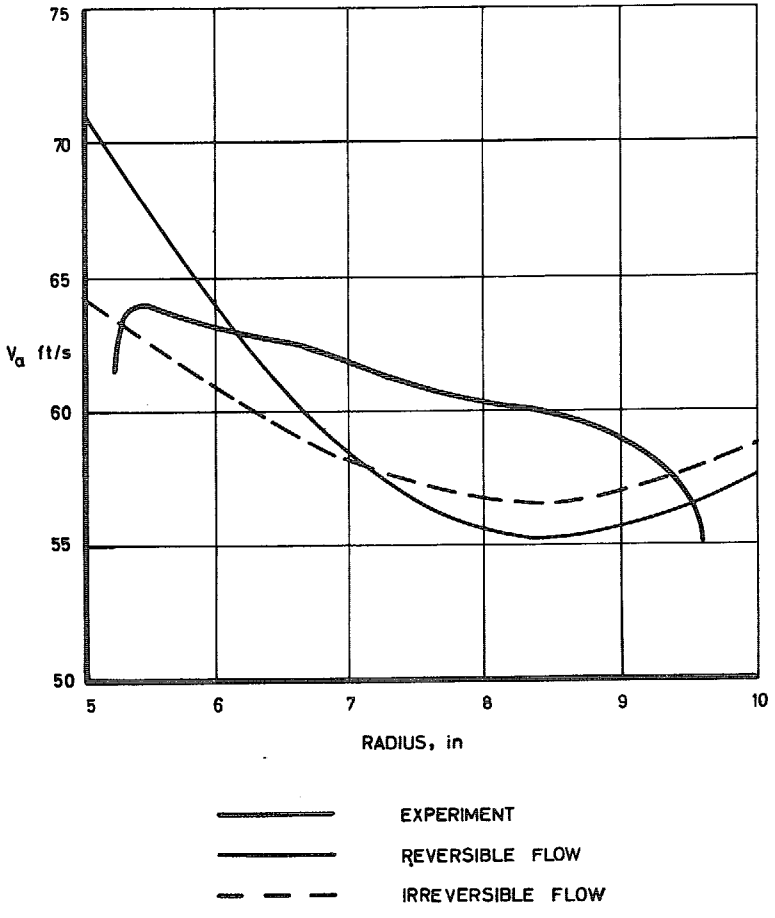

FIG. 13. Axial velocity profile after stator, $\overline{V}_a/U_m = 0{\cdot}65$.

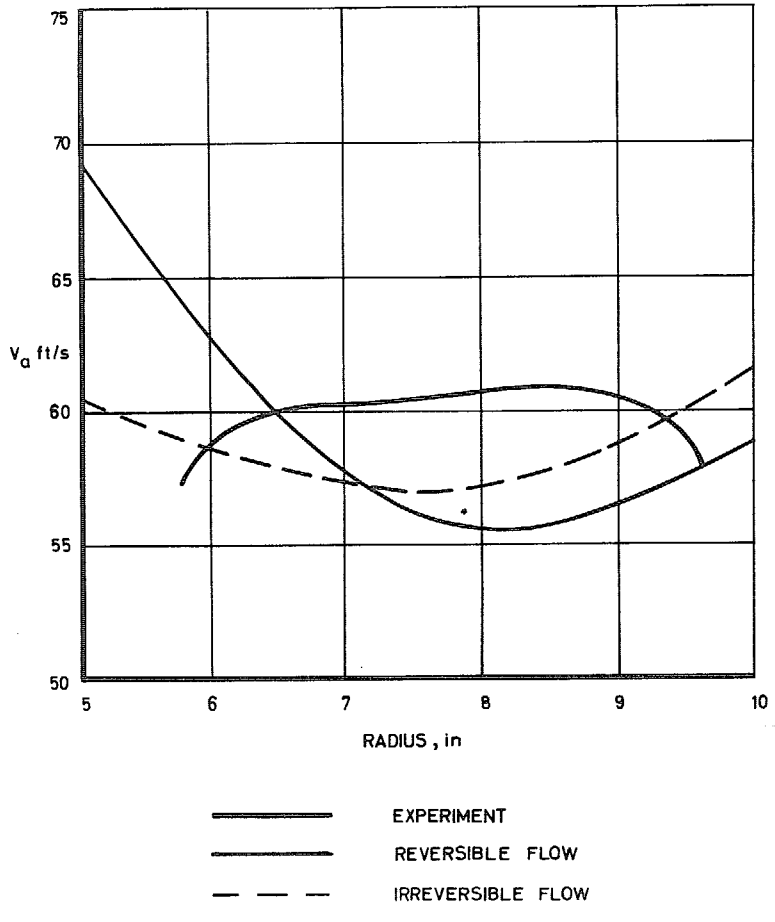

FIG. 14. Axial velocity profile far downstream, $\overline{V}_a/U_m = 0{\cdot}65$.

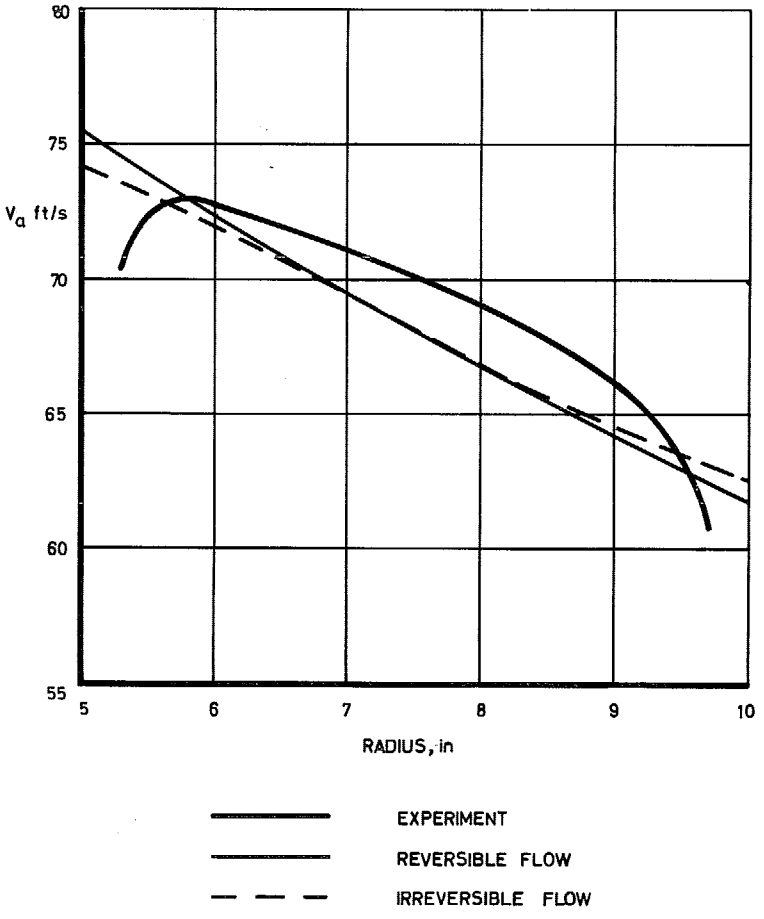

FIG. 15. Axial velocity profile after *IGV*, $\overline{V}_a/U_m = 0{\cdot}75$.

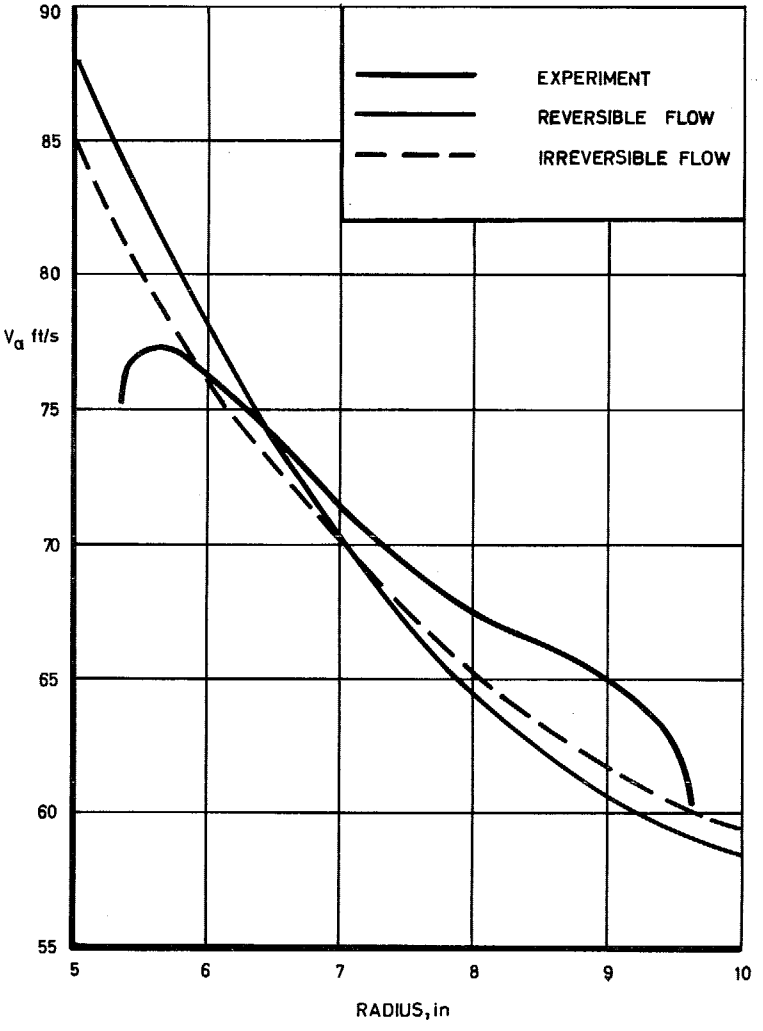

FIG. 16. Axial velocity profile after rotor, $\overline{V}_a/U_m = 0{\cdot}75$.

Printed in Wales for Her Majesty's Stationery Office by Allens Printers (Wales) Limited.
Dd. 129527. K5.

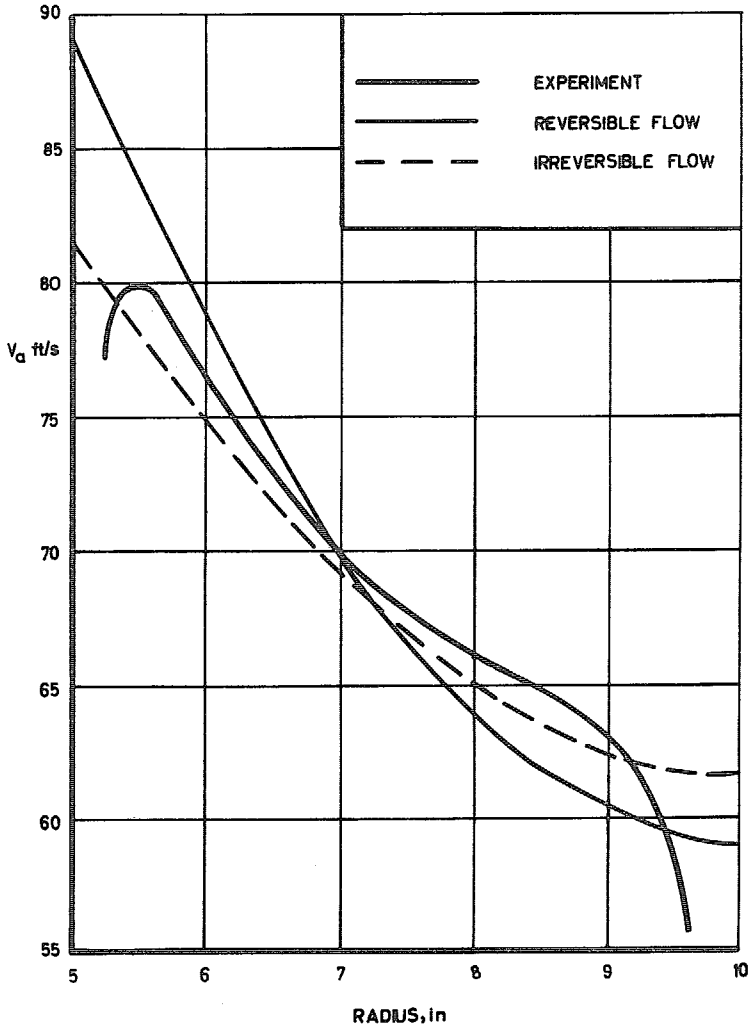

FIG. 17. Axial velocity profile after stator, $\bar{V}_a/U_m = 0{\cdot}75$.

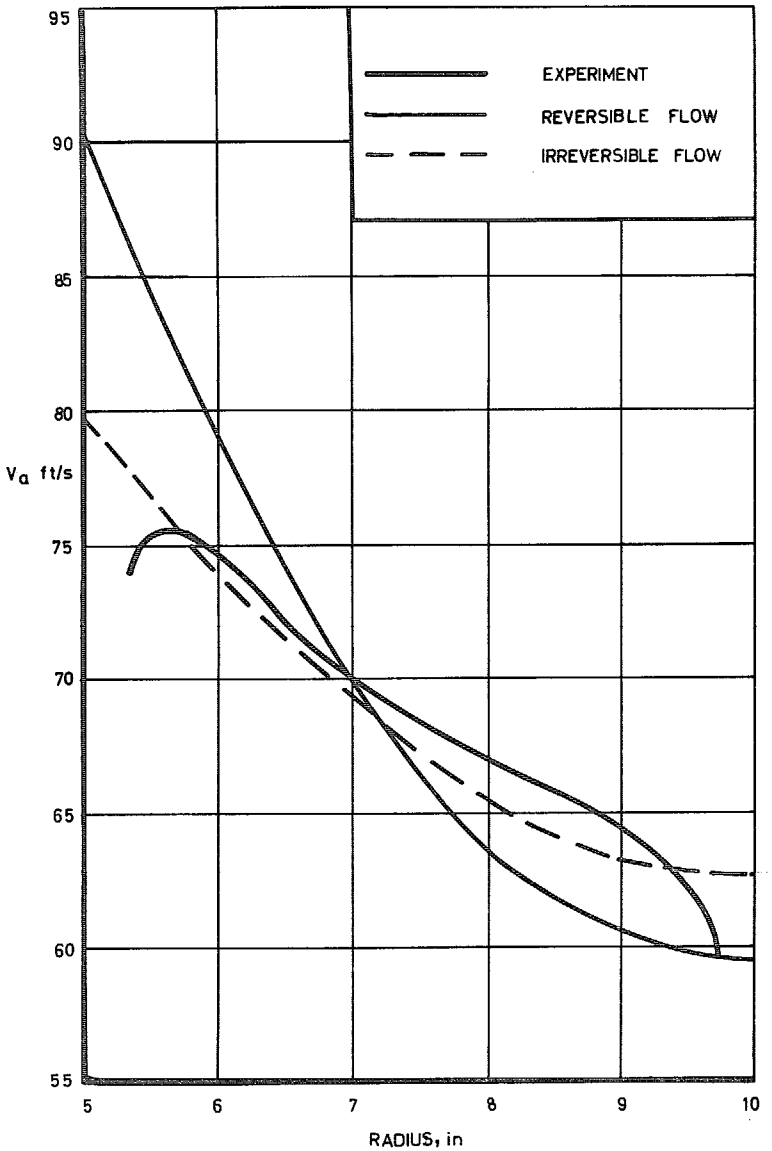

FIG. 18. Axial-velocity profile far downstream, $\bar{V}_a/U_m = 0{\cdot}75$.

Published by
HER MAJESTY'S STATIONERY OFFICE

To be purchased from
49 High Holborn, London W.C.1
423 Oxford Street, London W.1
13A Castle Street, Edinburgh 2
109 St. Mary Street, Cardiff CF1 1JW
Brazennose Street, Manchester 2
50 Fairfax Street, Bristol 1
258–259 Broad Street, Birmingham 1
7–11 Linenhall Street, Belfast BT2 8AY
or through any bookseller

S.O. Code No. 23-3509